

# Femtoscopic study of the $\Omega\alpha$ interaction in heavy-ion collisions

Faisal Etminan\*

*Department of Physics, Faculty of Sciences,  
University of Birjand, Birjand 97175-615, Iran and  
Interdisciplinary Theoretical and Mathematical Sciences  
Program (iTHEMS), RIKEN, Wako 351-0198, Japan*

(Dated: December 11, 2024)

The two-particle momentum correlation between the Omega-baryon ( $\Omega$ ) and the  ${}^4\text{He}(\alpha)$  in high-energy heavy ion collisions is explored. Such correlations as an alternative source of information can help us further understand the interaction between  $\Omega$  and nucleons (N).  $\Omega\alpha$  potentials in the single-folding potential approach are constructed by employing two different available  $\Omega N$  interactions in  ${}^5S_2$  channel, i.e, one is based on the (2 + 1)-flavor lattice QCD simulations near the physical point by the HAL QCD collaboration, and the other is based on the meson exchanges with effective Lagrangian, where in the latter case coupled channels effect is considered. It is found that the correlation functions at small size source depends on the potential model used. This implicitly means that at high density nuclear medium,  $\Omega\alpha$  momentum correlation could drive the feature of  $\Omega N$  interactions. Moreover, by extracting the scattering length and the effective range from obtained  $\Omega\alpha$  potentials, the correlation functions are calculated within the Lednicky-Lyuboshits (LL) formalism. It is shown that since the  $\Omega\alpha$  has large interaction range, the LL formula leads to different results at small source sizes.

## I. INTRODUCTION

The spin-2 Omega-nucleon ( $\Omega N$ ) state with  $S = -3$  is expected to lack a repulsive core since the Pauli exclusion principle does not act between quarks in this channel [1]. The theoretical improvement of the HAL QCD Collaboration methods [2–6] coupled with progress of high performance computing facilities provide the obtaining hadron-hadron interactions

---

\* [fetminan@birjand.ac.ir](mailto:fetminan@birjand.ac.ir)

at nearly physical quark masses from first principle lattice QCD simulations [7–10]. In the case of  $\Omega N$  system, they report a strongly attractive interaction in the  ${}^5S_2$  channel [11].

Moreover, in Ref. [12] Sekihara, Kamiya and Hyodo have developed a model based on the meson exchanges with effective Lagrangians to investigate the origin of the attraction in the  $\Omega N$  interaction in the  ${}^5S_2$  channel. They formulated an equivalent local potential for  $\Omega N$   ${}^5S_2$  interaction that reproduces  $\Omega N$   ${}^5S_2$  scattering length  $7.4 \pm 1.6$  fm at the time range  $t/a = 11$  of the lattice simulations nearly physical quark masses [11, 13] but with hadron masses tuned to the lattice simulations. The long range part of the potential is built on the exchanges of the  $\eta$  meson and correlated two mesons in the scalar-isoscalar channel (Known as " $\sigma$ "). The short-range part is constructed by the contact interaction. Furthermore, they considered the coupled channels effect on  $\Omega N$   ${}^5S_2$  interaction by adding the box diagrams with intermediate  $\Lambda\Xi$ ,  $\Sigma\Xi$  and  $\Lambda\Xi$  channels. They concluded that even though the elimination of these channels induces the energy dependence of the single-channel  $\Omega N$  interaction, this effect is not significant.

High energy heavy ion collisions are an excellent method for creating heavy hadrons and light (anti)nuclei, includes molecular states made of various hadrons or compact system. One method for studying the hadron-hadron interaction that is hard to investigate in scattering experiment is measuring the momentum correlation functions in high-energy collisions [14]. It can provide information on both the effective emission source and the interaction potential.

The first measurement of the proton- $\Omega$  correlation function [15, 16] in heavy-ion collisions by the STAR experiment at the Relativistic Heavy-Ion Collider (RHIC) [17, 18] favors the proton- $\Omega$  bound state hypothesis. In Ref. [18, 19] it is mentioned that the HAL QCD potential is the most consistent potentials with the LHC ALICE data.

As the next step in the femtoscopic analyses, the hadron-deuteron correlation functions would be promising [20]. The production of  $\Omega NN$  and  $\Omega\Omega N$  in ultra-relativistic heavy-ion collisions using the Lattice QCD  $\Omega N$ ,  $\Omega\Omega$  potentials has been studied in Ref. [21]. And very recently, the momentum correlation between  $\Lambda\alpha$  [22] and  $\Xi\alpha$  [23] are examined to shed light on the interaction between a hyperon and nucleons (N).

Therefore, motivated by the above discussions, in this work, I want to explore the  $\Omega\alpha$  correlation function in the relativistic heavy ion collisions to probe the nature of  $\Omega N$  interactions as an independent source of information. The purpose of this work is to give an illustration for what can be expected from measuring  $\Omega\alpha$  correlations. Since this is an

exploratory study, the techniques used are simple.

A Woods-Saxon type form for  $\Omega + \alpha$  potential is obtained in the framework of single-folding potential (SFP) approach. Because the  $\alpha$ -cluster has low compressibility feature, it is supposed that  $\Omega$  and  $\alpha$  pass in an effective  $\Omega\alpha$  potential. The effective  $\Omega + \alpha$  nuclear potential is estimated by the single-folding of nucleon density in the  $\alpha$ -particle and  $\Omega N$  interaction [24–27]. Next, the obtained  $\Omega\alpha$  potential is fitted to an analytical Woods-Saxon type function. Then, the Schrödinger equation is solved by the given  $\Omega\alpha$  potential as the input to calculate binding energy and scattering phase shift. And finally, the predictions on  $\Omega\alpha$  momentum correlation functions for given potentials are made by using the scattered wave functions of  $\Omega\alpha$  system.

The paper is organized in the following way: In Sec. II, HAL QCD and meson exchange  $\Omega N$  potentials are introduced. Also the single-folding potential approach is described briefly. In Sec. III the formalism for two-particle momentum correlation functions is briefly reviewed. Results and discussions for  $\Omega\alpha$  are presented in Sec. IV. The summary and conclusions are given in Sec. V.

## II. $\Omega N$ INTERACTIONS AND SINGLE-FOLDING POTENTIAL APPROACH

In this section, the HAL QCD and the meson exchanges  $\Omega N$  potentials which are used to find effective potential of  $\Omega + \alpha$  systems are described. Moreover, a short description of the SFP model is given [24, 27].

S-wave and spin 2  $\Omega N$  potential in configuration space is described by HAL QCD Collaboration with nearly physical quark masses [11]. The discrete lattice potential is fitted by an analytic function [1]

$$V_{\Omega N}^{HAL}(r) = b_1 e^{(-b_2 r^2)} + b_3 \left(1 - e^{-b_4 r^2}\right) \left(\frac{e^{-m_\pi r}}{r}\right)^2, \quad (1)$$

the Gauss functions describe the short-range and the Yukawa functions explain the meson exchange picture at medium to long-range distances of the potential. In Ref. [11], the discrete lattice results are fitted reasonably well,  $\chi^2/d.o.f \simeq 1$ , with four different sets of parameters  $b_{1,2,3}$  and  $b_4$ , they are given in Table 1 of Ref. [11]. Where each set of parameters corresponds to the imaginary-time slices  $t/a = 11, 12, 13, 14$  and  $a = 0.0846$  fm is the lattice spacing. Pion mass in Eq. (1) is taken from the lattice simulation,  $m_\pi = 146$  MeV. For

this potential, the scattering length, effective range and binding energy are  $a_0^{\Omega N} = 5.30$  fm,  $r_0^{\Omega N} = 1.26$  fm and  $B^{\Omega N} = 1.54$  MeV respectively [11].

As mentioned in the Introduction, next  $\Omega N$  potential model developed by Sekihara, Kamiya and Hyodo [12] is the meson exchanges (MS) potential and it is given in configuration space by,

$$V_{\Omega N}^{ME}(r) = \frac{1}{4\pi r} \sum_{n=1}^9 C_n \left( \frac{\Lambda^2}{\Lambda^2 - \mu_n^2} \right)^2 \left[ \exp(-\mu_n r) - \frac{(\Lambda^2 - \mu_n^2)r + 2\Lambda}{2\Lambda} \exp(-\Lambda r) \right], \quad (2)$$

where the cutoff parameter  $\Lambda = 1$  GeV,  $\mu_n = 100 n$  MeV and the parameters  $C_n$  are given by the real part of the last column in Table V of Ref. [12].

In Fig. 1, the  $\Omega N$  potential for HAL QCD in Eq. (1) at the imaginary-time distances  $t/a = 11, 12, 13, 14$  [11] and meson exchanges model [12] are depicted. Fig. 1 reveals a qualitative difference between these two models. Therefore, it is desirable to find out how these differences are embodied in the  $\Omega\alpha$  two-particle momentum correlation functions.

The effective  $\Omega + \alpha$  nuclear potential is approximated by the single-folding model

$$V_{\Omega\alpha}(r) = \int \rho(r') V_{\Omega N}(|\mathbf{r} - \mathbf{r}'|) d\mathbf{r}', \quad (3)$$

where  $V_{\Omega N}(|\mathbf{r} - \mathbf{r}'|)$  is  $\Omega N$  potential between the  $\Omega$  particle at  $\mathbf{r}'$  and the nucleon at  $\mathbf{r}$  [24, 26, 27]; moreover,  $\rho(r')$  is the nucleon density function in  $\alpha$ -particle at a distance  $\mathbf{r}'$  from its center-of-mass where can be taken as [28],

$$\rho(r') = 4 \left( \frac{4\beta}{3\pi} \right)^{3/2} \exp\left(-\frac{4}{3}\beta r'^2\right), \quad (4)$$

$\beta$  is a constant and it is defined by the rms radius of  ${}^4\text{He}$ , i.e.,  $r_{r.m.s} = \frac{3}{\sqrt{8\beta}} = 1.47$  fm [28]. The integration in Eq. (3) is over all space where  $\rho(r')$  is defined.

### III. TWO-PARTICLE CORRELATION FUNCTION

Two-particle correlation function formalism has been explained in detail in various publications such as [14, 29–32]. Here, only the essential formulae are provided. The two-particle momentum correlation function  $C_q$  is defined by Koonin-Pratt (KP) formula [32]

$$C(q) = \int d\mathbf{r} S(\mathbf{r}) |\Psi^{(-)}(\mathbf{r}, \mathbf{q})|^2, \quad (5)$$

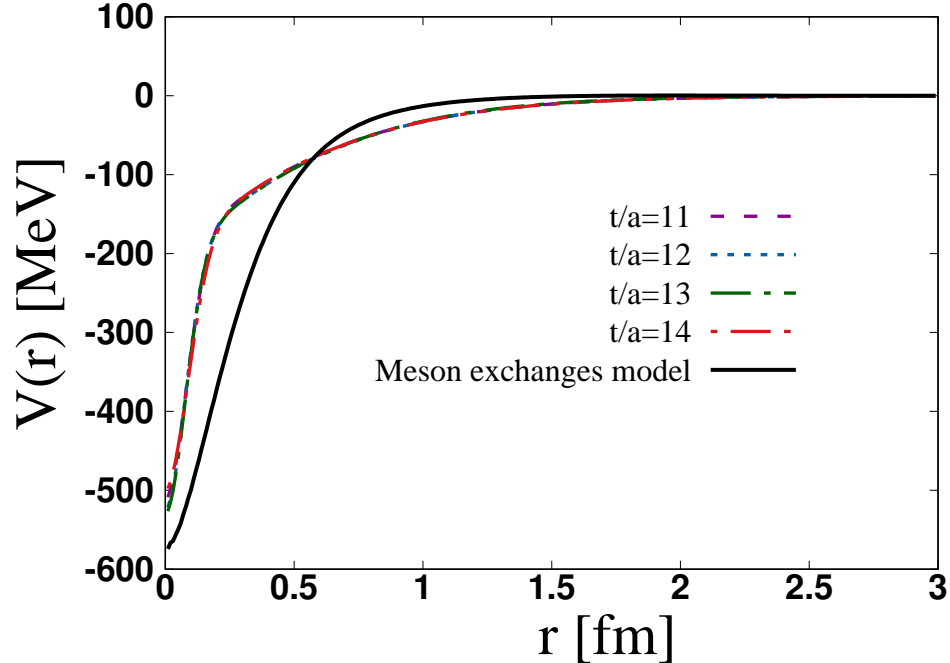


FIG. 1:  $\Omega N$  potentials as functions of the distance between  $\Omega$  and  $N$ . HAL QCD  $\Omega N$  potential,  $V_{\Omega N}^{HAL}$  in Eq. (1) at the imaginary-time distances  $t/a = 11, 12, 13, 14$  are shown by parametrization from Ref. [11] to compare with  $\Omega N$  potential based on the meson exchanges model (solid black line),  $V_{\Omega N}^{ME}$  in Eq. (2) from Ref. [12]. It should be mentioned that the HAL potentials are only in  ${}^5S_2$  channel but in the case of ME potential model the coupled channels effects are imposed on  $\Omega N$   ${}^5S_2$  interaction.

where  $S(r) = \exp\left(-\frac{r^2}{4R^2}\right) / (4\pi R^2)^{3/2}$  is a single particle source function that it is assumed to be spherical and static Gaussian with source size (source radius)  $R$ . The relative Gaussian source function  $S(r)$  defines the distribution of the  $\Omega\alpha$  pair production at the relative distance  $r$ . If  $R_\Omega$  and  $R_\alpha$  being the source size of the single  $\Omega$  and  $\alpha$  emissions, respectively, then the effective radius of the source is determined by  $R = \sqrt{(R_\Omega^2 + R_\alpha^2)}/2$  [14, 23]. The relative wave function  $\Psi^{(-)}$  contains only the S-wave interaction effect. The resulting correlation function can be written as

$$C(q) = 1 + \int_0^\infty 4\pi r^2 dr S(r) [|\psi(q, r)|^2 - |j_0(qr)|^2], \quad (6)$$

where  $j_{l=0}(qr) = \sin(qr)/qr$  is the spherical Bessel function and  $\psi(k, r)$  is the S-wave scattering wave function. For a given two-body  $\Omega\alpha$  potential it can be obtained straightforwardly by solving the Schrödinger equation.

When the source size is much larger than the interaction range, it is possible to employ the asymptotic behaviour of the wave function,  $\psi(q, r) \rightarrow j_0(qr) + f(q) \exp(iqr)/r$ , which leads to much more simple formula for the correlation function in the scattering length and the effective range, that is usually called the Lednický-Lyuboshits (LL) approach [33],

$$C_{LL}(q) = 1 + \frac{|f(q)|^2}{2R^2} F_0\left(\frac{r_0}{R}\right) + \frac{2\text{Re} f(q)}{\sqrt{\pi}R} F_1(2qR) - \frac{\text{Im} f(q)}{R} F_2(2qR), \quad (7)$$

where  $f(q) \approx 1/(-1/a_0 + r_0q^2/2 - iq)$  is scattering amplitude which can be calculated with the effective range expansion (ERE) formula Eq. (9). Further,  $F_1(x) = \int_0^x dt e^{t^2-x^2}/x$ ,  $F_2(x) = (1 - e^{-x^2})/x$ , and the factor  $F_0(x) = 1 - x/(2\sqrt{\pi})$  is a correction for the deviation of the true wave function from the asymptotic form [32, 33].

#### IV. NUMERICAL RESULTS

*Single folding  $\Omega\alpha$  potential.*-  $\Omega\alpha$  potential is obtained by solving Eq. (3) and, the resultant potentials are depicted in Fig. 2 for HAL QCD (at the imaginary-time distances  $t/a = 11$ ) and meson exchanges model potentials. The HAL potential is more attractive than the MS potential almost at all distances. The former is much deeper than the latter and more slowly goes to zero. But, in both cases, the interaction ranges are about 3 fm, although, it is slightly bigger than 3 fm for HAL potential.

For phenomenological application and calculation of observables, such as scattering phase shifts and binding energies, I fit  $V_{\Omega\alpha}(r)$  to a Wood-Saxon form using the function that is given by Eq. (8) (motivated by common Dover-Gal model of potential [34]) with three parameters,  $V_0$ ,  $R$  and  $c$ ,

$$V_{\Omega\alpha}^{fit}(r) = -V_0 \left[ 1 + \exp\left(\frac{r-R}{c}\right) \right]^{-1}, \quad (8)$$

where  $V_0$  is known as the depth parameter,  $R = 1.1A^{1/3}$  with  $A$  being the mass number of the nuclear core, i.e  $\alpha$  ( $A = 4$ ) and  $c$  is known as the surface diffuseness. By using the fit functions (solid lines in Fig 2) as input, the Schrödinger equation was solved in the infinite volume to extract binding energy and scattering observables from the asymptotic behavior of the wave function. Fig. 3 shows  $\Omega\alpha$  phase shifts  $\delta_0$  calculated with model of HAL QCD at  $t/a = 11$  and meson exchanges potentials for comparison. The phase shift behaviour for both cases shows an attractive interaction even to form a bound state with a binding energy of about 24 MeV for HAL potential, and about 7.5 MeV for MS potential.

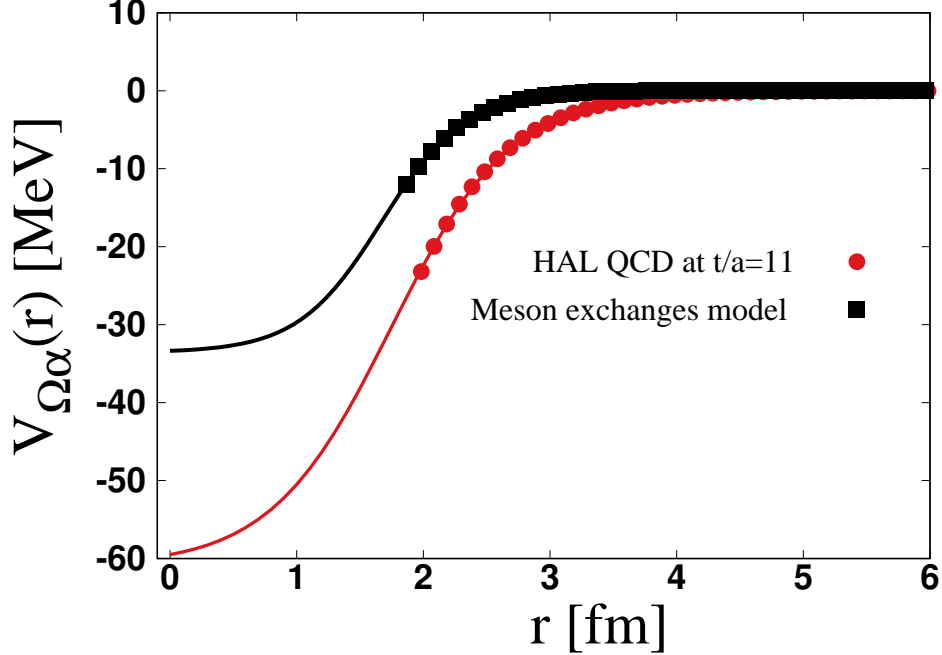


FIG. 2:  $V_{\Omega\alpha}(r)$ , the resultant single-folding potential as functions of distance between  $\Omega$  and  $\alpha$ . Potentials are obtained by solving Eq. (3) using  $\Omega N$  potential models of HAL QCD at  $t/a = 11$  (red circle) and meson exchanges model (black square). The corresponding  $\Omega N$  potentials are depicted in Fig. 1. In both cases, the solid lines show the fitting of  $V_{\Omega\alpha}(r)$  by using  $V_{\Omega\alpha}^{fit}(r)$  in Eq. (8). The results of the fit and the corresponding parameters are summarized in Table I.

Low-energy part of  $\Omega\alpha$  phase shifts in Fig. 3 provides the scattering length and the effective range by employing the ERE formula up to the next-leading-order (NLO),

$$q \cot \delta_0 = -\frac{1}{a_0} + \frac{1}{2}r_0q^2 + \mathcal{O}(q^4). \quad (9)$$

The fit parameters, scattering length, effective range and binding energy  $B_{\Omega\alpha}$ , with HAL and ME potentials are given in Table I. The fit functions Eq. (8) by these parameters are plotted in Fig. 2 by solid lines. As quoted in the caption of Table I, the numbers within parentheses correspond to the calculations by using  $\Omega$  mass derived by the lattice simulations [11], where they are slightly bigger than experimental masses. Since, by increasing the mass, the contribution of repulsive kinetic energy will decrease and finally lead to slightly deeper binding energies. Moreover, binding energies,  $B_{\Omega^-\alpha^{++}}$  ( $B_{\Omega\alpha}$ ), with (without) Coulomb interactions are given. A Coulomb potential due to a uniformly charged sphere is included.

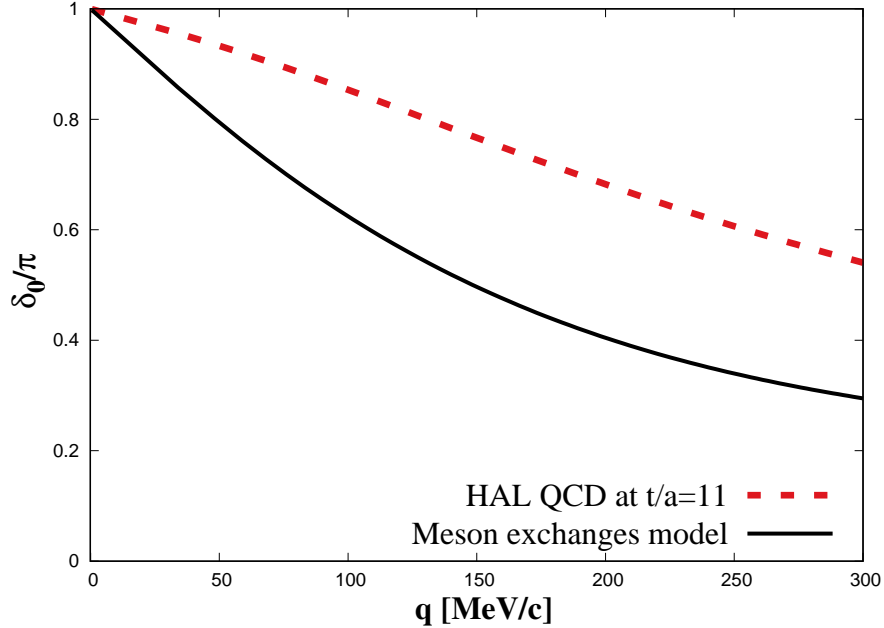


FIG. 3: The normalized  $\Omega\alpha$  phase shifts  $\delta_0/\pi$  as functions of the relative momentum  $q = \sqrt{2\mu E}$  ( $\mu$  is the reduced mass of  $\Omega\alpha$  system) using HAL QCD at  $t/a = 11$  (dashed red line) and meson exchanges model (solid black line) potentials.

TABLE I: The fit parameters of  $\Omega\alpha$  potential in Eq. (8) and the corresponding low-energy parameter, scattering length  $a_0$ , effective range  $r_0$  and binding energy  $B_{\Omega\alpha}$ , are given for HAL at  $t/a = 11$  and ME model of potentials. The results have been obtained by using the experimental masses of  $\alpha$  and  $\Omega$ , 3727.38 MeV/c and 1672.45 MeV/c respectively.

Furthermore, the results corresponding to  $\Omega$  mass value derived by the HAL QCD Collaboration 1711.5 MeV/c are given within parentheses.  $B_{\Omega^-\alpha^{++}}$  ( $B_{\Omega\alpha}$ ) is the binding energy with (without) Coulomb potential. In order to get a comprehensive evaluation, the experimental ERE parameters for neutron-neutron are  $(a_0, r_0) = (-18.5, 2.80)$  fm.

Model	$V_0$ (MeV)	$R$ (fm)	$c$ (fm)	$a_0$ (fm)	$r_0$ (fm)	$B_{\Omega\alpha}$ (MeV)	$B_{\Omega^-\alpha^{++}}$ (MeV)
$t/a = 11$	61.0	1.74	0.47	0.79(0.63)	2.81(5.80)	22.9(23.3)	24.2(24.6)
Meson exchange	33.6	1.67	0.33	2.65(2.60)	1.30(1.28)	6.4(6.6)	7.5(7.7)

$\Omega\alpha$  correlation function.- In order to calculate the two-particle correlations from KP formula, Eq. (6), I used the "Correlation Analysis tool using the Schrödinger Equation" (CATS) [35]. For given an interaction potential and an emission source of any form [36],



CATS is designed to calculate the correlation function.

$\Omega\alpha$  correlation functions from two  $\Omega\alpha$  potentials using KP formula (6) for three different source sizes,  $R = 1, 3$  fm and 5 fm are calculated and depicted in Fig. 4, where the choice is motivated by values suggested by analyses of the  $\Lambda\alpha$  correlation function [22]. Since the charge radius of the  $\alpha$  particle is about 1.68 fm [37], the source radius of  $R = 1$  fm, may seem small for the emission of the  $\alpha$  particle. But, as discussed in Ref. [35], the term  $4\pi r^2 S(r)$  in Eq. (6) describes the probability distribution of the relative distance  $r$  where the relative source function  $S(r)$  has the Gaussian width  $\sqrt{2}R$  [14, 23]. Correspondingly, with the source size  $R = 1$  fm, the mean distance between the emitted pair can be about  $\langle r \rangle = 4R/\sqrt{\pi} \sim 2.26$  fm that is sufficiently larger than the value of parameter  $R$ .

The results with Coulomb attraction are shown by dash-dotted red lines for HAL QCD potential and dashed black lines for meson exchanges potentials in Fig. 4. Once we include the Coulomb interaction between the negatively charged  $\Omega$  and the positively charged  $\alpha$ , a strong enhancement of  $C(q)$  at small  $q$  is introduced by the long-range attraction. At large source, the distinction of two potentials is smeared by the Coulomb attraction. The pure Coulomb result, when the strong interaction is switched off, is also illustrated in Fig. 4.

Also, it can be seen from Fig. 4 that in the area of low momentum  $q \lesssim 100$  MeV/c, the results for two potentials are different. According to Fig. 2, the HAL potential model is more attractive than ME potential model, thus it gives enhancement of  $C_{\Omega\alpha}(q)$ . But it is rather difficult to get this conclusion from Fig. 1. Nevertheless, with the increase of the source size ( $R = 3$  and 5 fm), the difference between the  $C_{\Omega\alpha}(q)$ s decreases until they are almost the same for  $R = 5$  fm. Therefore, the future measurement of  $\Omega\alpha$  correlation function from a small source at small relative momentum, can be substantially constrained by  $\Omega N$  interaction at high densities.

By employing the scattering length and the effective range of the two models of potentials given in Table I,  $\Omega\alpha$  correlation functions is calculated by using LL formula (Eq. 7), and the results are compared with the ones from KP formula in Fig. 5 for three different source sizes  $R = 1, 3$  and 5 fm. Figure 5 demonstrates that for  $R = 1$  fm, the LL formulation produces significant different results compared with the KP formula at low momentum region. In principle, the LL formula can not be a good approximation where the source size is smaller than the interaction range (for interactions that include nuclei, it can be about  $\gtrsim 3$  fm) [22]. On the other hand, the LL approximation is consistent with KP formula for relatively large

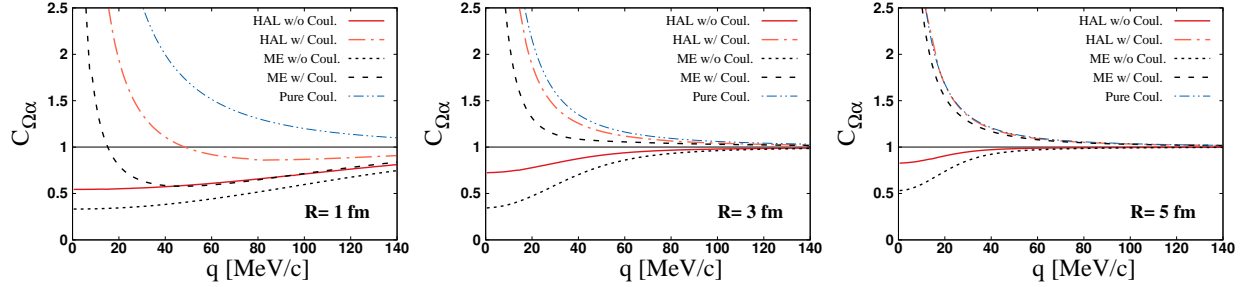


FIG. 4:  $\Omega\alpha$  correlation functions for three different source sizes. The solid and dash-dotted red lines are the results from the HAL QCD ( $t/a = 11$ ) potentials, without (w/o) and with (w/) Coulomb potential, respectively. The dotted and dashed black lines are the results of meson exchanges potentials, without and with Coulomb potential, respectively. For comparison, the pure Coulomb result, when the strong interaction is switched off, is presented by the dot-dash-dotted blue thin line for comparison.

source sizes, i.e.  $R \geq 3$  fm. Note that in Fig. 5, only the strong interaction is switched on.

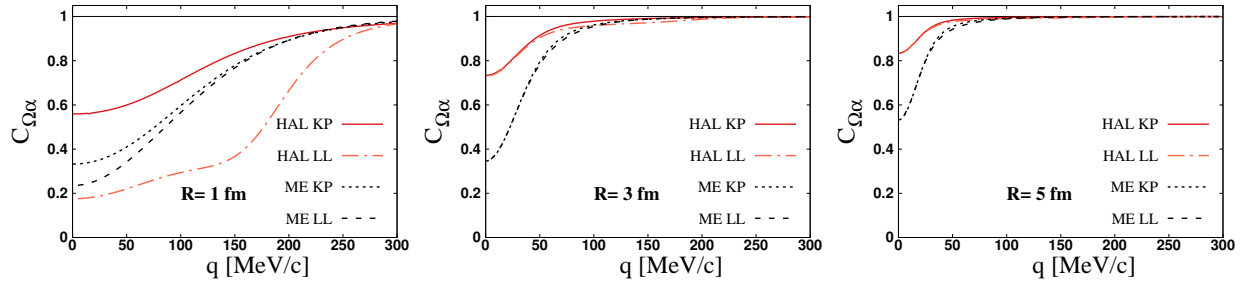


FIG. 5:  $\Omega\alpha$  correlation functions for three different source sizes. The solid and dash-dotted red lines are the results of the HAL QCD ( $t/a = 11$ ) potentials with the KP (Eq. (6)) and LL (Eq. (7)) relations, respectively. The dotted and dashed black lines are the results of meson exchanges potentials with the KP and LL relations, respectively. The Coulomb interaction is switched off.

## V. SUMMARY AND CONCLUSIONS

In the present paper, the  $\Omega\alpha$  potential is made from two available  $\Omega N$  interactions, i.e., first principles HAL QCD HAL and developed meson exchange potentials, in the latter potential, the coupled channels effect is considered.  $\Omega + \alpha$  potentials were obtained by using SFP model and they were fitted by Woods-Saxon type functions. The numerical results

showed that  $\Omega + \alpha$  potentials based on HAL potential is much deeper than the one based on ME potential by binding energies around 24 and 7.5 MeV, respectively. In both cases, the interaction ranges are about 3 fm.

I applied femtoscopy technique to predict  $\Omega\alpha$  momentum correlation functions in the high-energy collisions looking for an additional and alternative source of knowledge relevant to the  $\Omega N$  interaction. Employing two  $\Omega\alpha$  potentials, correlation functions are calculated using KP formula for three different source sizes,  $R = 1, 3$  fm and 5 fm. The difference of potentials appears in the correlation functions by small source size around 1 – 3 fm, with and without considering the Coulomb interactions, while for source size  $R \gtrsim 5$  fm the correlation functions tended to become the same for both  $\Omega\alpha$  potentials with Coulomb interactions. In all cases without Coulomb potential, the differences still remain significant at short distance. In conclusion, since the correlation functions are sensitive to  $\Omega\alpha$  potentials behavior and Coulomb interactions, we could get important information about the effects of  $\Omega$  particle in dense nuclear medium.

Furthermore, the binding energy, scattering length and effective range were calculated by solving the Schrödinger equation using the fitted  $\Omega\alpha$  potentials as the input for HAL and ME potential. Next, correlation functions were examined within the Lednicky-Lyuboshits approach and compared with the results of KP formula when Coulomb interaction is switched off. It was seen, as expected, that the LL formula by small source (1 fm) significantly differs from KP formula in the low-momentum region.

Last but not least, in this theoretical study, the selection of source sizes  $R = 1, 3$ , and 5 fm is based on previous studies of the two-hadron correlation function in  $pp$  collisions and heavy ion collisions [22, 23]. The Koonin-Pratt formula, Eq. (6), is valid while the two correlated particles can be considered as well separated point-like particle. In the case of composite particle like  $\alpha$ , since there is a possibility of simultaneous formation of alpha particle the effective source size must be larger than those with single hadron emissions [38–40]. Therefore, basically we are facing a 5-body problem of two protons, two neutrons and  $\Omega$  and a emergence of alpha particle and production of  $\Omega$ - $\alpha$  correlation take place at same time, this effect will be considered in future works. I hope that these theoretical studies could help to design experiments at FAIR [41], NICA, and J-PARC HI [42] in future.

## ACKNOWLEDGEMENT

I thank Yuki Kamiya and Asanosuke Jinno for useful discussions, comments and sharing some data with me. I am grateful to the authors and maintainers of ”*Correlation Analysis tool using the Schrödinger Equation*” (CATS) [35], a modified version of which is used for calculations in this work. Discussions during the long-term workshop, HHIQCD2024, at Yukawa Institute for Theoretical Physics (YITP-T-24-02), were useful as I finished this work.

- 
- [1] F. Etminan *et al.* (HAL QCD Collaboration), Spin-2  $N\Omega$  dibaryon from lattice QCD, [Nucl. Phys. A \*\*928\*\*, 89 \(2014\)](#), special Issue Dedicated to the Memory of Gerald E Brown (1926-2013).
  - [2] N. Ishii, S. Aoki, and T. Hatsuda, Nuclear force from lattice QCD, [Phys. Rev. Lett. \*\*99\*\*, 022001 \(2007\)](#).
  - [3] N. Ishii *et al.* (HAL QCD Collaboration), Hadron–hadron interactions from imaginary-time Nambu–Bethe–Salpeter wave function on the lattice, [Phys. Lett. B \*\*712\*\*, 437 \(2012\)](#).
  - [4] S. Aoki, B. Charron, T. Doi, T. Hatsuda, T. Inoue, and N. Ishii, Construction of energy-independent potentials above inelastic thresholds in quantum field theories, [Phys. Rev. D \*\*87\*\*, 034512 \(2013\)](#).
  - [5] S. Kenji *et al.* (HAL QCD Collaboration),  $\Lambda\Lambda$  and  $N\Xi$  interactions from lattice QCD near the physical point, [Nucl. Phys. A \*\*998\*\*, 121737 \(2020\)](#).
  - [6] F. Etminan, K. Sasaki, and T. Inoue, Coupled-channel  $\Lambda_c K^+ - p D_s$  interaction in the flavor SU(3) limit of lattice QCD, [Phys. Rev. D \*\*109\*\*, 074506 \(2024\)](#).
  - [7] S. Gongyo *et al.* (HAL QCD Collaboration), Most strange dibaryon from lattice QCD, [Phys. Rev. Lett. \*\*120\*\*, 212001 \(2018\)](#).
  - [8] Y. Lyu, H. Tong, T. Sugiura, S. Aoki, T. Doi, T. Hatsuda, J. Meng, and T. Miyamoto, Dibaryon with Highest Charm Number near Unitarity from Lattice QCD, [Phys. Rev. Lett. \*\*127\*\*, 072003 \(2021\)](#).
  - [9] Y. Lyu, T. Doi, T. Hatsuda, Y. Ikeda, J. Meng, K. Sasaki, and T. Sugiura, Attractive  $N-\phi$  interaction and two-pion tail from lattice QCD near physical point, [Phys. Rev. D \*\*106\*\*, 074507](#)

- (2022).
- [10] Y. Lyu, S. Aoki, T. Doi, T. Hatsuda, Y. Ikeda, and J. Meng, Doubly Charmed Tetraquark  $T_{cc}^+$  from Lattice QCD near Physical Point, *Phys. Rev. Lett.* **131**, 161901 (2023).
- [11] T. Iritani *et al.*,  $N\Omega$  dibaryon from lattice QCD near the physical point, *Phys. Lett. B* **792**, 284 (2019).
- [12] T. Sekihara, Y. Kamiya, and T. Hyodo,  $N\Omega$  interaction: Meson exchanges, inelastic channels, and quasibound state, *Phys. Rev. C* **98**, 015205 (2018).
- [13] Doi, Takumi *et al.*, Baryon interactions from lattice QCD with physical quark masses – Nuclear forces and  $\Xi\Xi$  forces –, *EPJ Web Conf.* **175**, 05009 (2018).
- [14] S. Cho, T. Hyodo, D. Jido, C. M. Ko, S. H. Lee, S. Maeda, K. Miyahara, K. Morita, M. Nielsen, A. Ohnishi, *et al.*, Exotic hadrons from heavy ion collisions, *Prog. Part. Nucl. Phys.* **95**, 279 (2017).
- [15] K. Morita *et al.*, Probing multistrange dibaryons with proton-omega correlations in high-energy heavy ion collisions, *Phys. Rev. C* **94**, 031901 (2016).
- [16] M. P. i Méndez, A. Parreño, and J. Torres-Rincon,  $p\Omega$  femtoscopy using baryon-baryon effective potentials (2024), [arXiv:2409.16747 \[nucl-th\]](https://arxiv.org/abs/2409.16747).
- [17] J. Adam *et al.* (STAR Collaboration), The proton- $\Omega$  correlation function in Au + Au collisions at  $s_{NN} = 200$  GeV, *Phys. Lett. B* **790**, 490 (2019).
- [18] S. Acharya *et al.* (ALICE Collaboration), Unveiling the strong interaction among hadrons at the LHC, *Nature* **588**, 232 (2020).
- [19] L. Fabbietti, V. M. Sarti, and O. V. Doce, Study of the Strong Interaction Among Hadrons with Correlations at the LHC, *Annu. Rev. Nucl. Part. Sci.* **71**, 377 (2021).
- [20] S. Acharya *et al.* (ALICE Collaboration), Exploring the Strong Interaction of Three-Body Systems at the LHC, *Phys. Rev. X* **14**, 031051 (2024).
- [21] L. Zhang, S. Zhang, and Y.-G. Ma, Production of  $\Omega NN$  and  $\Omega\Omega N$  in ultra-relativistic heavy-ion collisions, *Eur. Phys. J. C* **82**, 1 (2022).
- [22] A. Jinno, Y. Kamiya, T. Hyodo, and A. Ohnishi, Femtoscopic study of the  $\Lambda\alpha$  interaction, *Phys. Rev. C* **110**, 014001 (2024).
- [23] Y. Kamiya, A. Jinno, T. Hyodo, and A. Ohnishi, Theoretical study on  $\Xi\alpha$  correlation function (2024), [arXiv:2409.13207 \[nucl-th\]](https://arxiv.org/abs/2409.13207).

- [24] G. Satchler and W. Love, Folding model potentials from realistic interactions for heavy-ion scattering, *Phys. Rep.* **55**, 183 (1979).
- [25] K. S. Myint and Y. Akaishi, Double-Strangeness Five-Body System, *Prog. Theor. Phys.* **117**, 251 (1994).
- [26] T. Miyamoto *et al.* (HAL QCD),  $\Lambda_c N$  interaction from lattice QCD and its application to  $\Lambda_c$  hypernuclei, *Nucl. Phys. A* **971**, 113 (2018).
- [27] F. Etminan and M. M. Firoozabadi, Simple Woods-Saxon type form for  $\Omega\alpha$  and  $\Xi\alpha$  interactions using folding model, *Chin. Phys. C* **44**, 054106 (2020).
- [28] Y. Akaishi, *Cluster Models and Other Topics*, International review of nuclear physics (World Scientific, 1986).
- [29] S. E. Koonin, Proton pictures of high-energy nuclear collisions, *Phys. Lett. B* **70**, 43 (1977).
- [30] S. Pratt, Pion interferometry of quark-gluon plasma, *Phys. Rev. D* **33**, 1314 (1986).
- [31] K. Morita, T. Furumoto, and A. Ohnishi,  $\Lambda\Lambda$  interaction from relativistic heavy-ion collisions, *Phys. Rev. C* **91**, 024916 (2015).
- [32] A. Ohnishi, K. Morita, K. Miyahara, and T. Hyodo, Hadron-hadron correlation and interaction from heavy-ion collisions, *Nucl. Phys. A* **954**, 294 (2016).
- [33] R. Lednicky and V. L. Lyuboshits, Final State Interaction Effect on Pairing Correlations Between Particles with Small Relative Momenta, *Yad. Fiz.* **35**, 1316 (1981).
- [34] C. Dover and A. Gal,  $\Xi$  Hypernuclei, *Ann. Phys.* **146**, 309 (1983).
- [35] D. Mihaylov, V. Sarti, O. Arnold, L. Fabbietti, B. Hohlweger, and A. Mathis, A femtosopic Correlation Analysis Tool using the Schrödinger equation (CATS), *Eur. Phys. J. C* **78**, 394 (2018).
- [36] D. Mihaylov and J. González González, Novel model for particle emission in small collision systems, *Eur. Phys. J. C* **83**, 590 (2023).
- [37] J. J. Krauth *et al.*, Measuring the  $\alpha$ -particle charge radius with muonic helium-4 ions, *Nat.* **589**, 527 (2021).
- [38] S. Mrówczyński and P. Słoń, Hadron-deuteron correlations and production of light nuclei in relativistic heavy-ion collisions, *Acta Phys. Pol. B* **51**, 1739 (2020).
- [39] S. Bazak and S. Mrówczyński, Production of  ${}^4\text{Li}$  and  $p$ - ${}^3\text{He}$  correlation function in relativistic heavy-ion collisions, *Eur. Phys. J. A* **56**, 193 (2020).

- [40] S. Mrówczyński and P. Słoń, Deuteron-deuteron correlation function in nucleus-nucleus collisions, [Phys. Rev. C \*\*104\*\*, 024909 \(2021\)](#).
- [41] T. Ablyazimov *et al.*, Challenges in QCD matter physics –The scientific programme of the Compressed Baryonic Matter experiment at FAIR, (CBM), [Eur. Phys. J. A \*\*53\*\*, 60\(2017\) \(2017\)](#).
- [42] K. Ozawa *et al.*, The J-PARC heavy ion project, [EPJ Web Conf. \*\*271\*\*, 11004 \(2022\)](#).